ARTICLES

Journal of Semiconductors
(2019) 40, 012804
doi: 10.1088/1674-4926/40/1/012804

Heteroepitaxial growth of thick α-Ga_2O_3 film on sapphire (0001) by MIST-CVD technique

Tongchuan Ma, Xuanhu Chen, Fangfang Ren, Shunming Zhu, Shulin Gu, Rong Zhang, Youdou Zheng, and Jiandong Ye†

Research Institute of Shenzhen and School of Electronics Science and Engineering, Nanjing University, Nanjing 210093, China

Abstract: The 8 μm thick single-crystalline α-Ga_2O_3 epilayers have been heteroepitaxially grown on sapphire (0001) substrates via mist chemical vapor deposition technique. High resolution X-ray diffraction measurements show that the full-widths-at-half-maximum (FWHM) of rocking curves for the (0006) and (10-14) planes are 0.024° and 0.24°, and the corresponding densities of screw and edge dislocations are 2.24×10^6 and 1.63×10^9 cm^{-2}, respectively, indicative of high single crystallinity. The out-of-plane and in-plane epitaxial relationships are [0001] α-Ga_2O_3//[0001] α-Al_2O_3 and [11-20] α-Ga_2O_3//[11-20] α-Al_2O_3, respectively. The lateral domain size is in micron scale and the indirect bandgap is determined as 5.03 eV by transmittance spectra. Raman measurement indicates that the lattice-mismatch induced compressive residual strain cannot be ruled out despite the large thickness of the α-Ga_2O_3 epilayer. The achieved high quality α-Ga_2O_3 may provide an alternative material platform for developing high performance power devices and solar-blind photodetectors.

Key words: ultra-wide bandgap semiconductor; chemical vapor deposition; epitaxy; gallium oxide

Citation: T C Ma, X H Chen, F F Ren, S M Zhu, S L Gu, R Zhang, Y D Zheng, and J D Ye, Heteroepitaxial growth of thick α-Ga_2O_3 film on sapphire (0001) by MIST-CVD technique[J]. *J. Semicond.*, 2019, 40(1), 012804. http://doi.org/10.1088/1674-4926/40/1/012804

1. Introduction

Gallium oxide (Ga_2O_3), a representative ultra-wide bandgap (UWBG) semiconducting material, has attracted considerable attention in the applications of power electronic devices and solar-blind photodetectors owing to its unique properties, including an ultra-wide bandgap of about 4.9 eV and a high breakdown electric field of 8 MV/cm[1, 2]. As is well known, Ga_2O_3 has six different phases, among which, the monoclinic β-phase is the most thermodynamically stable phase and most studies in the last decade have focused on the use of β-Ga_2O_3[3, 4]. Various growth techniques have been proved to be effective methods for the preparation of β-Ga_2O_3 in forms of bulk[5], thin films[6–10] and nanostructures[11]. Power devices, including MOSFET[2], and Schottky diode[12], as well as solar-blind photodetectors[11] based on β-Ga_2O_3 have been reported with improving performance. In contrast, the other metastable phases are less studied but recently have drawn increasing attention due to their interesting properties. For instance, corundum-like α-phase Ga_2O_3 exhibits similar hexagonal structure and relatively small lattice mismatch with GaN, ZnO and sapphire substrates. It also offers a relatively large bandgap of about 5.1 eV, small electron effective mass, a higher breakdown field and a larger Baliga's figure of merit[13, 14]. The superior physical properties of α-Ga_2O_3, together with easy integration with other corundum structure functional oxides, such as Al, Cr, Fe oxides[15], allows the design and delivering of high performance solar-blind photodetector and power electronic devices.

The growth of α-Ga_2O_3 thin films have been realized by various means of metal–organic vapor phase epitaxy (MOCVD)[16], halide vapor phase epitaxy (HVPE)[17], mist-chemical vapor deposition and molecular beam epitaxy (MBE) techniques[18]. In particular, a high performance Schottky diode with a breakdown voltage over 1 kV and a small specific on-resistance of 2.5 mΩ·cm^2 has been achieved and a normally-off MOSFET has been first demonstrated based on α-Ga_2O_3 material grown by a mist-CVD system[19]. Therefore, the growth of highly crystalline α-Ga_2O_3 on an inexpensive sapphire substrate provides an alternative platform to realize high performance power devices. However, the in-plane lattice mismatch of 4.6% between α-Ga_2O_3 and the sapphire substrate, as well as the mismatch in the coefficient of thermal expansion, will build up strain within α-Ga_2O_3 epilayers, which will lead to lattice distortion and introduce dislocations. Owing to the heteroepitaxial growth, a thick α-Ga_2O_3 epilayer over 3 μm often suffers from the generation of cracks, which is not desirable as the drift layer of the Schottky diode in vertical configuration, which can operate at high voltages[20]. To this end, we have optimized the growth condition to produce a highly crystalline, crack-free α-Ga_2O_3 layer with a thickness up to 8 μm. The resultant thick α-Ga_2O_3 exhibits a relatively low screw dislocation density, a large crystalline domain size, and a large bandgap of about 5 eV. The lattice dynamics indicate the strain is fully relieved despite lattice mismatch.

2. Experiment

The growth procedures were conducted using a hot-wall type mist-CVD system as developed by Shinohara and Fujita[21]. The schematic of the mist-CVD system is shown in Fig. 1. The sapphire (0001) substrate was cleaned by acetone, ethanol and deionized water and dried by nitrogen. Gallium acetylacetonate [$(C_5H_7O_2)_3Ga$] solved in DI water (0.05 mol/L)

Correspondence to: J D Ye, yejd@nju.edu.cn
Received 1 AUGUST 2018; Revised 13 SEPTEMBER 2018.
©2019 Chinese Institute of Electronics

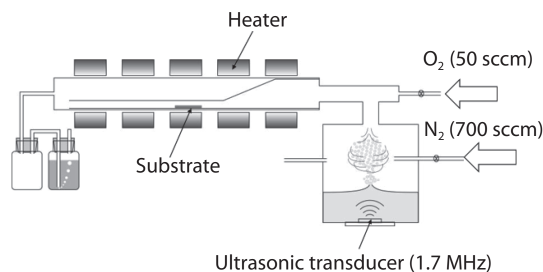

Fig. 1. Schematic illustration the mist-CVD system used for α-Ga_2O_3 epitaxy.

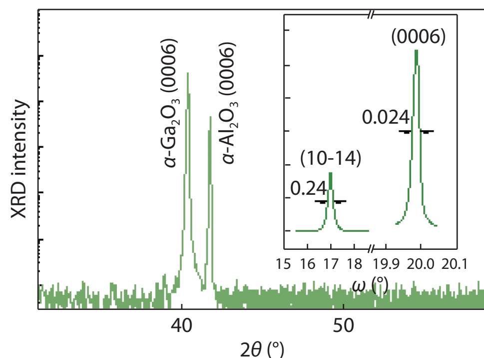

Fig. 2. (Color online) X-ray diffraction (XRD) $2\theta/\omega$ scan spectrum of the thick α-Ga_2O_3 epilayer. The inset displays the ω-scan rocking curves of (0006) and (10-14) planes under symmetric and skew-symmetric scan configuration, respectively.

with 1.5% HCl was used as Ga source. The solution was atomized into micron-sized particles by a 1.7 MHz ultrasonic transducer and then carried into the growth chamber by N_2 gas with a flow rate of 700 sccm. To eliminate the carbon contamination, a small fractional oxygen with a flow rate of 50 sccm was also introduced into the carrier gas. A right-trapezoid shaped quartz liner was designed to form a fine channel to improve the reaction efficiency of the reactants[22]. The atmospheric pressure was maintained for the growth period and the substrate temperature was kept at 500 °C. The thickness of the grown sample was determined to be 8 μm from the cross-section SEM and the corresponding growth rate was about 1 μm/ h.

The microstructures of α-Ga_2O_3 epilayers were characterized by high resolution X-ray diffraction (HRXRD) using a D8 advance system with a Cu Kα X-ray source and a high resolution of 0.0001°. Optical transmission spectra were recorded by a UV-visible near-IR scanning spectrophotometer (Lambda 950, PerkinElmer). Raman scattering and photoluminescence spectroscopy measurements were performed at room temperature using a Micro-Raman spectrometer system (Horiba JY T64000) in a backscattering configuration with a 514 nm Ar^+ laser as the excitation source. The laser was focused using a 100× objective for a spot size of ~2 μm in diameter and the excitation power was from 0.2 mW to avoid the laser heating effect. The surface morphology was investigated using atomic force microscopy (Asylum Research AFM).

3. Results and discussion

Fig. 2 shows the X-ray diffraction (XRD) $2\theta/\omega$ scan spectrum of the thick α-Ga_2O_3 epilayer. The spectrum is dominated by the diffraction peaks at 40.34° and 41.76°, which correspond to the (0006) planes of α-Ga_2O_3 epilayer and sapphire sub-

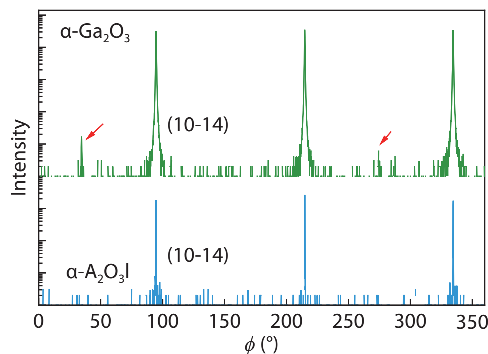

Fig. 3. (Color online) XRD Φ-scan measurement for the (10-14) plane of the α-Ga_2O_3 epilayer and α-Al_2O_3 substrate.

strate, respectively. The calculated lattice constant along the c-axis is 13.40 Å, consistent with that of the other reported values for α-Ga_2O_3. There are no other distinct diffraction peaks observed in the XRD pattern, indicating phase-pure single crystalline α-Ga_2O_3 with (0001) out-of-plane orientation has been achieved. The inset of Fig. 2 illustrates the ω scan rocking curves of (0006) and (10-14) planes under symmetric and skew-symmetric scan configuration, respectively. The full-width at half maximum (FWHM) of the ω scan rocking curves for (0006) planes is as narrow as 0.024° (86 arcsec). Similar to the hexagonal III-nitride and ZnO epilayers grown on sapphire substrates, lattice twist and tilt are directly related to the dislocation density and can be roughly evaluated from the broadening feature of the ω scan[23]. Normally, ω-scans of (000l) reflections are used to measure the lattice tilt from mixed or screw dislocations, while edge dislocations do not distort the (000l) planes as their Burgers vectors lie within those planes. Assuming the dislocations are randomly distributed, the dislocation density can be obtained from the relationship of $D_{\rm B} = \dfrac{\beta^2}{4.35b^2}$, where β is the FWHM of ω scan and b is the length of the Burgers vector[24]. This model has been used to calculate the density of edge and of screw dislocation densities in III-nitride and ZnO films, with separate equations involving the ω-FWHM of symmetric and asymmetric planes[23]. Following the same approach, the c-type screw dislocation density is estimated to be 2.24×10^6 cm^{-2}, given that the length of the Burgers vector is equal to the lattice constant of c for (0006) orientation. The low screw dislocation density indicates a small lattice tilt from the (0006) orientation[25]. In contrast, the ω-FWHM of (10-14) plane exhibits a larger value of 0.24°, and the corresponding dislocation density is estimated to be 1.63×10^9 cm^{-2} with a Burgers vector of 1/3(-2110), which is much higher than the screw dislocation density[25]. It can be understood that the in-plane lattice mismatch of 4.6% between α-Ga_2O_3 and α-Al_2O_3 will introduce strain within the initial growth stage and the strain relaxation in thick α-Ga_2O_3 leads to the generation of a large amount of a-type edge dislocations with twist crystalline domains.

Fig. 3 shows the result of XRD Φ-scan measurement for the (10–14) plane of the α-Ga_2O_3 epilayer and α-Al_2O_3 substrate. Predominant peaks with 120° intervals appear at the same rotational angle of Φ, suggesting the epitaxial α-Ga_2O_3 film has the same corundum structure as the substrate. The epitaxial relationship is $[0001]_{\alpha\text{-Ga2O3}}//[0001]_{\alpha\text{-Al2O3}}$ in the out-of-plane orientation and $[10\text{-}10]_{\alpha\text{-Ga2O3}}//[10\text{-}10]_{\alpha\text{-Al2O3}}$ in the in-plane orientation. Aside from the distinct peaks of three-fold rotational symmetry, very weak peaks are seen in the

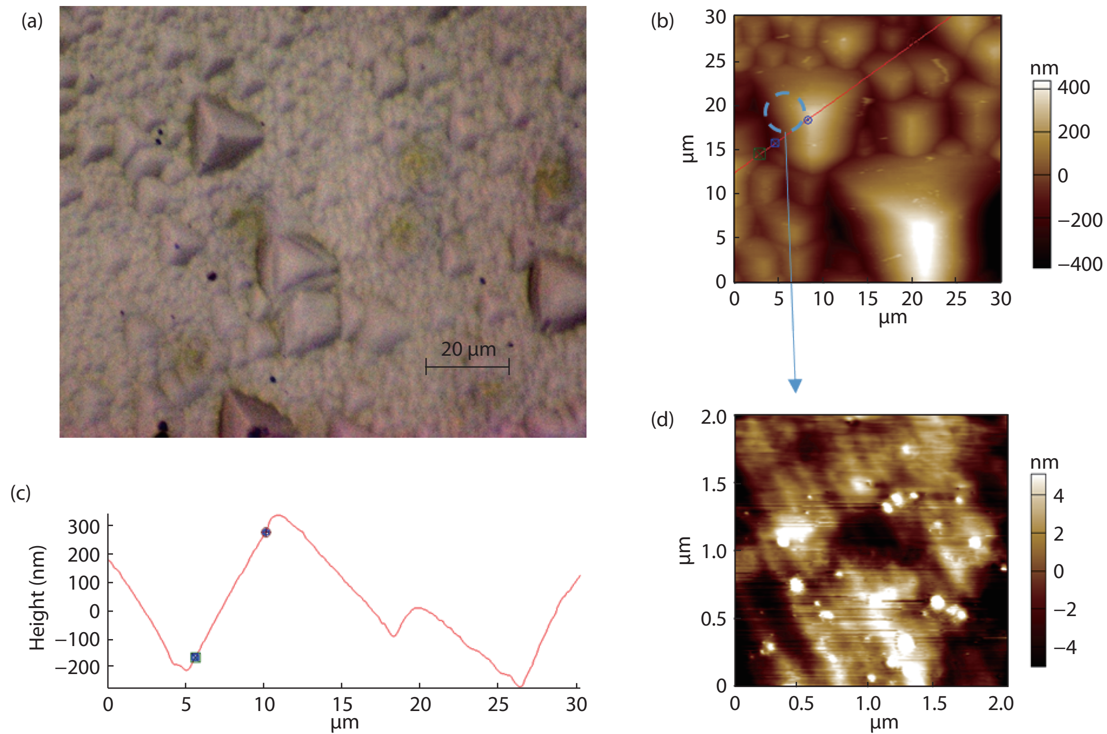

Fig. 4. (Color online) (a) Optical microscopic image. (b) Large-scale atomic force microscopic image of the α-Ga_2O_3 epilayer. (c) Cross-sectional profile of grain. (d) AFM image of side facet of grain.

α-Ga_2O_3 epilayer (marked by the red arrows in Fig. 3) at the positions rotated by 60° with respect to the predominant peaks. It means that a very small amount of 60°-twisted domains are formed during the epitaxial growth, which is expected to generate edge dislocations surrounding the twist boundaries of the rotational domains. The crystalline domains can be observed by the optical microscopic and atomic force microscopic (AFM) characterization as shown in Figs. 4(a) and 4(b), respectively. Determined from the optical microscopic image, the surface is crack-free but dominated by pyramid structures with different size distribution. The AFM image in Fig. 4(b) also clearly shows that a bunch of tetrahedron-structured grains dominates the surface morphology and the size of lateral coherent domain is in micron-scale. The cross-sectional profile of AFM shown in Fig. 4(c) shows that the angle between the side facet of the tetrahedron and the surface is about 6.05°, which is very close to the angle of 6.11° between the atomic planes of (0006) and (10-16). It indicates the side facets of tetrahedrons are in 10-16 orientation and exhibit a small roughness of 2.9 nm as shown in Fig. 4(d).

The optical transmittance spectrum of the α-Ga_2O_3 epilayer was recorded by using a c-plane sapphire substrate as reference and is shown in the inset of Fig. 5(a). A sharp absorption edge is observed at about 245 nm while the transmittance is low without the observable interference oscillations in the spectral range from near-ultraviolet to the visible region, which may suffer from a rough surface morphology. Typically, the optical bandgap can be evaluated by using the well-known Tauc rules of $(ahv)^n = A(hv - E_g)$, where the value of the exponent, n denotes the nature of the optical transitions[26]. Good linearity of $(ahv)^n$ versus hv is expected when n equals 1/2 for indirect allowed transition or n equals 2 for direct bandgap[10]. Fig. 5(a) shows the $(ahv)^{1/2}$ curve as a function of photon energy, hv for all samples derived from the original transmittance spectra. It is clear that the plot of $(ahv)^{1/2}$ versus hv exhibits an excellent linearity relationship with a smaller deviation error. The analysis unambiguously identified the indirect band structure of α-Ga_2O_3, in good agreement with the theoretical calculation results discussed earlier[10]. The indirect optical bandgap is determined to be 5.03 eV, which is larger than that of β-Ga_2O_3.

Raman scattering is a powerful and nondestructive approach to probe lattice dynamics and evaluate crystalline quality and strain status. Fig. 5(b) shows the Raman scattering spectra of α-Ga_2O_3 epilayer obtained in a backscattering configuration together with that of α-Al_2O_3 substrate for reference. The Raman peaks located at 218.1, 288.4, 328.5, 431.4, 570.3, 690.3 cm^{-1} are the Raman-allowed vibration modes of A_{1g}, E_g, E_g, E_g, E_g, A_{1g} and E_g, respectively, consistent with the theoretical calculation in Ref. [27]. As reported by R. Cusco *et al.*, the α-Ga_2O_3 with a rhombohedral structure belongs to the R3c space group and Raman active optical modes in the Brillouin zone center include $2A_{1g} + 5E_g$ in terms of Raman selection rule. The low-frequency A_{1g} mode at 218.1 cm^{-1} corresponds to Ga atoms vibrating against each other along the c-axis while the high-frequency A_{1g} mode at 570.3 cm^{-1} mainly involves the vibration of oxygen atoms perpendicular to the c-axis. The linewidth of the low-frequency A_{1g} is as narrow as 4.3 cm^{-1}, strongly suggesting the highly crystallinity of the epilayer. As compared with the frequencies obtained from DFT calculations, the measured Raman frequencies are higher[27]. This could be the result of the compressive residual strain in the α-Ga_2O_3 epilayer at the interface due to the in-plane lattice mismatch.

4. Conclusion

In summary, the 8-μm thick single-crystalline crack-free α-

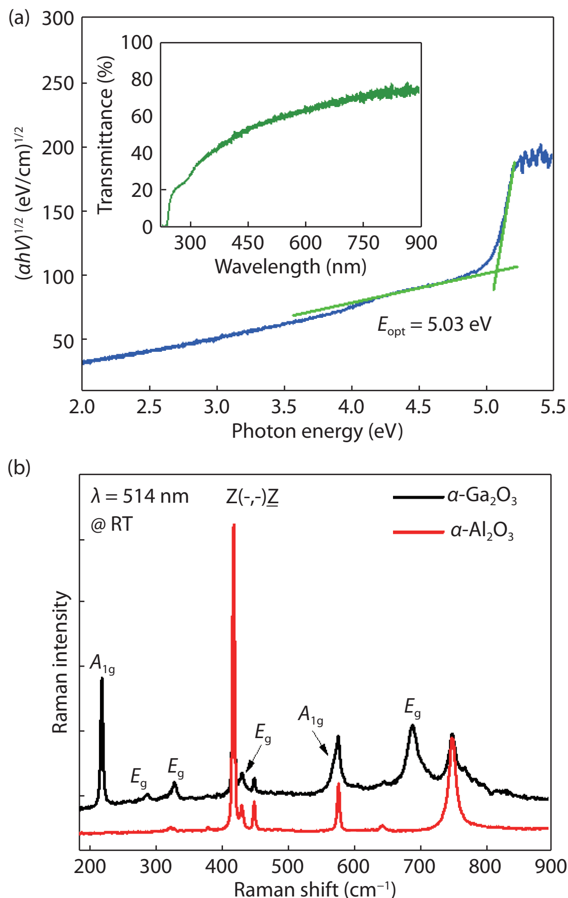

Fig. 5. (Color online) (a) The derived $(ahv)^{1/2}$ curve as a function of photon energy and the inset displays the optical transmittance spectrum. (b) Raman scattering spectra of the α-Ga_2O_3 epilayer and α-Al_2O_3 substrate.

Ga_2O_3 epilayers have been heteroepitaxially grown on sapphire (0001) substrates via the mist chemical vapor deposition technique. The resultant α-Ga_2O_3 has a low screw dislocation density of 2.24 × 10^6 cm^{-2} with very tiny lattice tilt from the (0006) orientation, while the 60°-twisted domains formed during the epitaxial growth leads to the generation of edge dislocations with a large density of about 1.63 × 10^9 cm^{-2}. The surface is crack-free but dominated by pyramid structures with domain size in micron-scale. The optical transition exhibits an indirect nature with an optical bandgap of 5.03 eV. Lattice dynamics reveal the high crystallinity of the thick epilayer with a compressive residual strain not fully relaxed at the interface. The achieved high quality α-Ga_2O_3 with unique properties may be an alternative to β-Ga_2O_3 in the application of power devices and solar-blind photodetectors.

Acknowledgements

This work was supported by the National Key Research and Development Project (No. 2017YFB0403003), Shenzhen Fundamental Research Project (Nos. 201773239, 201888588), the National Natural Science Foundation of China (Nos. 61774081, 61322403), State Key Laboratory of Wide-Bandgap Semiconductor Power Electric Devices (No. 2017KF001), the Natural Science Foundation of Jiangsu Province (No. BK20161401), the Six Talent Peaks Project in Jiangsu Province (Mo. 2014XXRJ001), the Fundamental Research Funds for the Central Universities (Nos. 021014380093, 021014380085).

References

[1] Varley J B, Weber J R, Janotti A, et al. Oxygen vacancies and donor impurities in β-Ga_2O_3. Appl Phys Lett, 2010, 97(14), 142106
[2] Higashiwaki M, Sasaki K, Kuramata A, et al. Gallium oxide (Ga_2O_3) metal–semiconductor field-effect transistors on single-crystal β-Ga_2O_3 (010) substrates. Appl Phys Lett, 2012, 100(1), 013504
[3] Playford H Y, Hannon A C, Barney E R, et al. Structures of uncharacterised polymorphs of gallium oxide from total neutron diffraction. Chemistry, 2013, 19(8), 2803
[4] Roy R, Hill V G, Osborn E F. Polymorphism of Ga_2O_3 and the System Ga_2O_3–H_2O. J Am Chem Soc, 1952, 74(3), 719
[5] Aida H, Nishiguchi K, Takeda H, et al. Growth of β-Ga_2O_3 single crystals by the edge-defined, film fed growth method. Jpn J Appl Phys, 2008, 47(11), 8506
[6] Mahmoud W E. Solar blind avalanche photodetector based on the cation exchange growth of β-Ga_2O_3/SnO_2 bilayer heterostructure thin film. Sol Energy Mater Sol Cells, 2016, 152, 65
[7] Guo D Y, Shi H Z, Qian Y P, et al. Fabrication of β-Ga_2O_3/ZnO heterojunction for solar-blind deep ultraviolet photodetection. Semicond Sci Technol, 2017, 32(3), 03LT01
[8] Zhao X, Wu Z, Guo D, et al. Growth and characterization of α-phase $Ga_{2-x}Sn_xO_3$ thin films for solar-blind ultraviolet applications. Semicond Sci Technol, 2016, 31(6), 065010
[9] Chen X, Xu Y, Zhou D, et al. Solar-blind photodetector with high avalanche gains and bias-tunable detecting functionality based on metastable phase alpha-Ga_2O_3/ZnO isotype heterostructures. ACS Appl Mater Interfaces, 2017, 9(42), 36997
[10] Li J, Chen X, Ma T, et al. Identification and modulation of electronic band structures of single-phase β-$(Al_xGa_{1-x})_2O_3$ alloys grown by laser molecular beam epitaxy. Appl Phys Lett, 2018, 113(4), 041901
[11] Zhao B, Wang F, Chen H, et al. Solar-blind avalanche photodetector based on single ZnO–Ga_2O_3 core-shell microwire. Nano Lett, 2015, 15(6), 3988
[12] Sasaki K, Higashiwaki M, Kuramata A, et al. Ga_2O_3 Schottky barrier diodes fabricated by using single-crystal β-Ga_2O_3 (010) substrates. IEEE Electron Device Lett, 2013, 34(4), 493
[13] Akaiwa K, Fujita S. Electrical conductive corundum-structured α-Ga_2O_3 thin films on sapphire with tin-doping grown by spray-assisted mist chemical vapor deposition. J Jpn J Appl Phys, 2012, 51, 070203
[14] Ito H, Kaneko K, Fujita S. Growth and band gap control of corundum-structured α-Ga_2O_3 thin films on sapphire by spray-assisted mist chemical vapor deposition. Jpn J Appl Phys, 2012, 51, 100207
[15] Kaneko K, Nomura T, Kakeya I, et al. Fabrication of highly crystalline corundum-structured α-$(Ga_{1-x}Fe_x)_2O_3$ alloy thin films on sapphire substrates. Appl Phys Express, 2009, 2, 075501
[16] Sun H, Li K H, Castanedo C G T, et al. HCl flow-induced phase change of α-, β-, and ε-Ga_2O_3 films grown by MOCVD. Cryst Growth Des, 2018, 18(4), 2370
[17] Yao Y, Okur S, Lyle L A M, et al. Growth and characterization of α-, β-, and ϵ-phases of Ga_2O_3 using MOCVD and HVPE techniques. Mater Res Lett, 2018, 6(5), 268
[18] Kumaran R, Tiedje T, Webster S E, et al. Epitaxial Nd-doped alpha-$(Al_{(1-x)}Ga_{(x)})_2O_3$ films on sapphire for solid-state waveguide lasers. Opt Lett, 2010, 35(22), 3793
[19] Fujita S, Oda M, Kaneko K, et al. Evolution of corundum-structured III-oxide semiconductors: Growth, properties, and devices. Jpn J Appl Phys, 2016, 55(12), 1202A3
[20] Oda M, Kaneko K, Fujita S, et al. Crack-free thick (~5 μm) α-Ga_2O_3 films on sapphire substrates with α-$(Al,Ga)_2O_3$ buffer layers. Jpn J Appl Phys, 2016, 55(12), 1202B4
[21] Shinohara D, Fujita S. Heteroepitaxy of corundum-structured α-Ga_2O_3 thin films on α-Al_2O_3 substrates by ultrasonic mist chemic-

al vapor deposition. Jpn J Appl Phys, 2008, 47(9), 7311
[22] Kawaharamura T. Physics on development of open-air atmospheric pressure thin film fabrication technique using mist droplets: Control of precursor flow. Jpn J Appl Phys, 2014, 53(5), 05FF08
[23] Moram M A, Vickers M E. X-ray diffraction of III-nitrides. Rep Prog Phys, 2009, 72(3), 036502
[24] Zheng X H, Chen H, Yan Z B, et al. Determination of twist angle of in-plane mosaic spread of GaN films by high-resolution X-ray diffraction. J Cryst Growth, 2003, 255(1/2), 63
[25] Kaneko K, Kawanowa H, Ito H, et al. Evaluation of misfit relaxation in α-Ga_2O_3 epitaxial growth on α-Al_2O_3 substrate. Jpn J Appl Phys, 2012, 51, 020201
[26] Davis E A, Mott N F, et al. Conduction in non-crystalline systems V. Conductivity, optical absorption and photoconductivity in amorphous semiconductors. Philos Mag A, 1970, 22(179), 0903
[27] Cusco R, Domenech-Amador N, Hatakeyama T, et al. Lattice dynamics of a mist-chemical vapor deposition-grown corundum-like Ga_2O_3 single crystal. J Appl Phys, 2015, 117(18), 185706